Impact of cutting tool wear on residual stresses induced during turning of a 15-5 PH stainless steel

F. Clavier, F. Valiorgue, C. Courbon, M. Dumas, J. Rech, A. Van Robaeys, F. Lefebvre, A. Brosse, H. Karaouni

Available online at www.sciencedirect.com

ScienceDirect

Procedia CIRP 00 (2019) 000–000

www.elsevier.com/locate/procedia

5th CIRP CSI 2020

Impact of cutting tool wear on residual stresses induced during turning of a 15-5 PH stainless steel

F.Clavier[a]*, F.Valiorgue[a], C.Courbon[a], M.Dumas[a,b], J.Rech[a] , A.Van Robaeys[b], F.Lefebvre[c], A.Brosse[d], H.Karaouni[e]

[a] *University of Lyon, ENISE, LTDS CNRS UMR 5513, 58 Rue Jean Parot, 42000 Saint-Etienne, France*
[b] *Airbus Helicopters, Aéroport Marseille Provence, 13725 Marignane, France*
[c] *CETIM, 7 Rue de la presse, 42952 Saint-Etienne, France*
[d] *Framatome, 10 Rue Juliette Récamier, 69456 Lyon, France*
[e] *SAFRAN Tech, Rue des Jeunes-Bois, 78772 Magny-les-Hameaux, France*
* Corresponding author. Tel.: +33 4 77 43 84 00. *E-mail address:* florent.clavier@enise.fr

Abstract

Finish turning is one of the key operations governing the residual stresses below the machined surface. The residual stress state depends on the cutting conditions and on the selected cutting tool system, i.e. macro geometry, cutting edge preparation as well as tool grade. However, tool wear often affects the interaction between the tool and the workpiece leading to severe modifications of the residual stress state. This work aims at investigating the influence of cutting tool wear on the surface integrity in longitudinal turning of a 15-5PH stainless steel. First, an experimental sensitivity study is performed to assess the effect of various wear modes on the residual stresses. Then a numerical model has been developed to understand the experimental observations and connect them to the thermomechanical loadings and local data within the near surface. The impact on residual stresses of three types of wear were tested (flank face wear, rake face wear and adhesion on the cutting edge) with the same cutting condition (V_c =120m/min, a_p = 0.2 mm and f = 0.2 mm.rev^{-1}). Based on the experiment, the numerical simulation proposes to observe the impact of wear on thermomechanical loadings by simulated a tool with a rounded cutting edge, a crater on the rake face and high flank face contact length. It follows that the impact of the rake face wear is extremely low, contrary to the rounded edge or the flank face wear which increased the contact length and significantly impact the loadings.

Keywords: Tool wear; residual stresses; turning; surface integrity

1. Introduction

The aircraft industry is extremely demanding on the fatigue resistance of its safety components. During the manufacturing of a part, machining processes will induce a residual stress state in the external functional layer. The state in this layer plays a major role in the fatigue resistance of mechanical parts [1–5].

This paper will present the consequence of the tool wear on the surface residual stress state. In the past, some numerical models have been developed to predict residual stresses induced by machining process[6–10]. Moreover, some experimental work has been performed to observe the wear of the tools and its effects on the residual stress state [11–13]. However, phenomenon that impact the residual stresses with the evolution of the wear are still not completely understood.

Numerical studies has already been performed to observe the impact of wear types [11, 14, 15] but the influence of each wear types on the thermomechanical loading is unclear.

This paper proposes to assess the consequences of tool wear on the surface residual stress state. This study will focus on the impact of tool wear on the residual stresses of the 15-5 PH martensitic stainless steel used for helicopters.

First, some experimental investigations have been realized to study the impact of different wear nodes. Then, a numerical

model has been created to observe the evolution of the thermomechanical loading by the increasing of the tool wear and have a better understanding of the experimental surface residual stresses.

2. Experimental investigations

2.1. Wear modes

Experimental tests have been performed in order to observe the impact of the wear on the residual stress. The cutting insert reference is DNMG 150608 PM 4325 from Sandvik. The insert is a carbide tool with a CVD Ti (C, N) – Al2O3 coating and is used with the following cutting conditions: V_c = 120m.min^{-1}, f = 0.2 mm.rev^{-1}, a_p = 0.2mm, dry cutting

The studied workmaterial is the 15-5 PH stainless steel H1025, which is a martensitic Precipitation-Hardening material with chromium, nickel, copper and with the following mechanical properties: hardness = 35 HRC; tensile strength = 1070 MPa; yield strength = 1000 MPa.

To represent all the possible wear modes, three tools were selected with a specific profile (Fig. 1):

- The first one is a new tool (Tool 1).
- The second tool (tool 2) represents a low wear status, with mainly flank wear but with a high adhesion of the cut material on the cutting edge. This adhesion modifies the micro-geometry of the cutting edge.
- The third tool (tool 3) represents a critical wear on the rake face with a limited wear on the flank face.
- The last tool (tool 4) has a totally collapsed flank face.

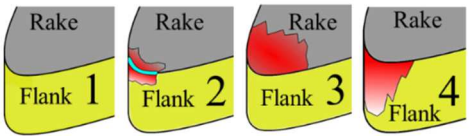

Fig. 1. Wear modes

2.2. Tool with high adhesion (Type 2)

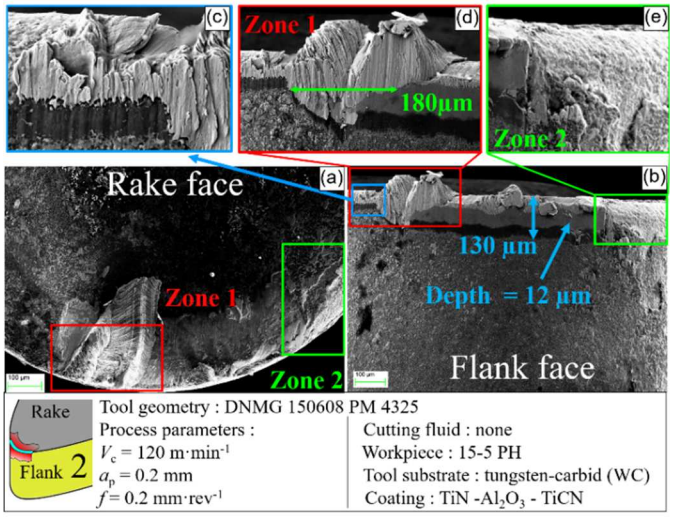

Fig. 2. SEM analysis of tool with high adhesion on the cutting edge

The wear of this tool is low, but the adhesion of the material is extremely important.

Two significant wear zones can be observed on this tool (Fig.2):

- The Zone 1 (Fig. 2.d)) corresponds to the interaction zone between the extreme surface of the workpiece and the tool. This surface was strain hardened by the previous machining revolution and creates a more severe wear by notching the tool. In this case, the wear probably reached the substrate. However, this zone isn't directly in contact with the final surface and doesn't have a significant impact on the surface integrity.
- The second zone (Fig. 2.e)) is created by the chip on the rake face, which is extremely abrasive (also due to high levels of strain hardening). The friction between the chip and the tool forms an important wear, down to the substrate. But, like the other zone, this one will not have an impact on the machined surface.

For the remaining part of the tool tip, the 15-5 PH material transfer is important and located mostly on the cutting edge (Fig. 2.c)) and related to the cyclic formation of a built-up edge. This type of mechanism is induced by the large contact pressures generated by this stainless steel and promoted by the relatively low cutting speed. The cutting edge is indeed a zone extremely propitious to the concentration of adhered material due to the sliding velocity of the material tending to zero [16].

Besides changing the local tribological conditions, i.e. friction coefficient and heat transfer, this material transfer may have an impact on the cutting edge making it sharper or rounder and thus potentially impacting the residual stress state.

2.3. Tool with a large rake face wear (Type 3)

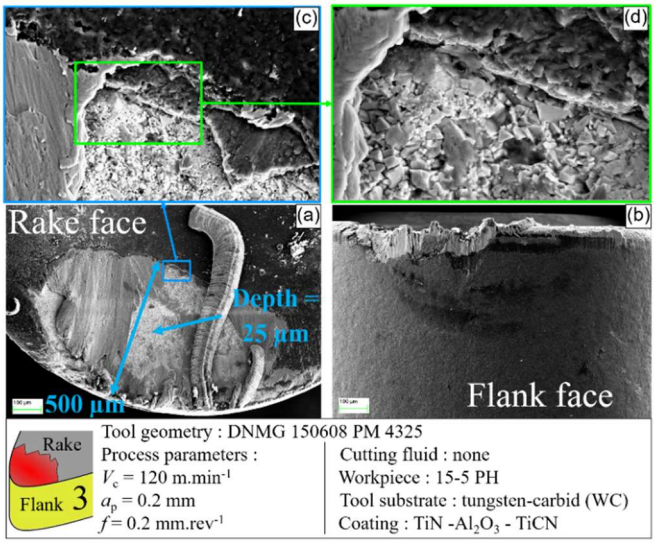

Fig. 3. SEM analysis of the tool with a large rake face wear

This wear is due to the interaction between the chip and the tool, which generate higher temperatures and contact pressures compared to the flank face. These critical parameters are especially responsible for the delamination of the different coatings [17] (Fig. 3.c)).

The wear is present in a large zone where the coating was totally pull out (Fig. 3.a)) and the tungsten-carbide grains are observable (Fig. 3.d)). A significant wear on the rake face like this one could have an impact on the material flow in the secondary shear zone and change the cutting forces. Indeed, the lack of coating will increase the adhesion of the chip on the face and may consequently impact the surface stresses.

This tool will allow to observe the impact of the rake face only and to assess its importance in the generation of surface residual stresses.

2.4. Tool with collapsed flank face (Type 4)

The flank face of this tool totally collapsed due to an important stress and created a large and deep crater. The work material was then able to accumulate and led to extremely severe conditions at the interface (Fig. 4). Here again, the friction and heat partition laws are completely different and impossible to determinate. The micro-geometry of this tool is far from the initial state and will be one of the critical parameters regarding the generation of residual stress state.

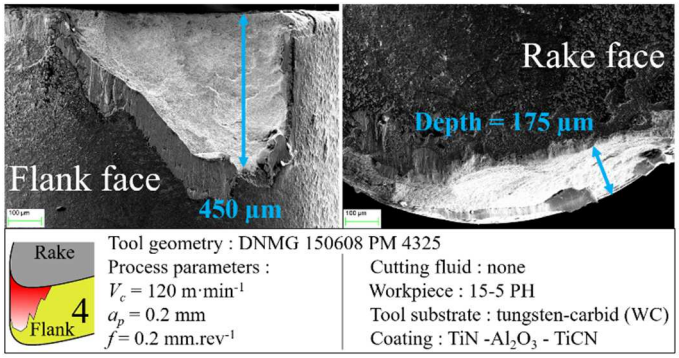

Fig. 4. SEM analysis of the tool with high flank face wear

The flank face is directly in contact will the final surface and represent the most suitable area for the impact on the residual stresses.

These tools represent the majority of the wear that occurs in the industry during the last stage of the tool's life. Investigating the residual stresses it induced will allow to understand which type of wear is critical.

3. Residual stresses after using the worn tools

3.1. Measuring set-up

All the diffraction measurements presented in this article have been performed using an iXRD system provided by the PROTO Company and the conditions use in [8].

A MG40 head was used and equipped with a 2-mm diameter collimator and electrolytic attacks were performed between each measure to observe a different depth.

3.2. Impact on the residual stresses

Fig. 5. plots the residual stresses of each tool configuration presented before. The impact of each wear types seems similar in the axial (Fig. 5.a)) and in the circumferential (Fig. 5.b)) direction.

Tool with adhesion (Fig. 5 – type 2)

The residual stress gradient of the tool with adhesion on the cutting edge is relatively similar to the gradient of the new tool, but with a reduced compression peak and a lower affected depth. This adhesion of the 15-5 PH creates an interaction zone with completely different properties compared to a new tool. The friction coefficient, the heat transfer and the local stresses are expected to be different leading to a change in the balance between thermal and mechanical loadings.

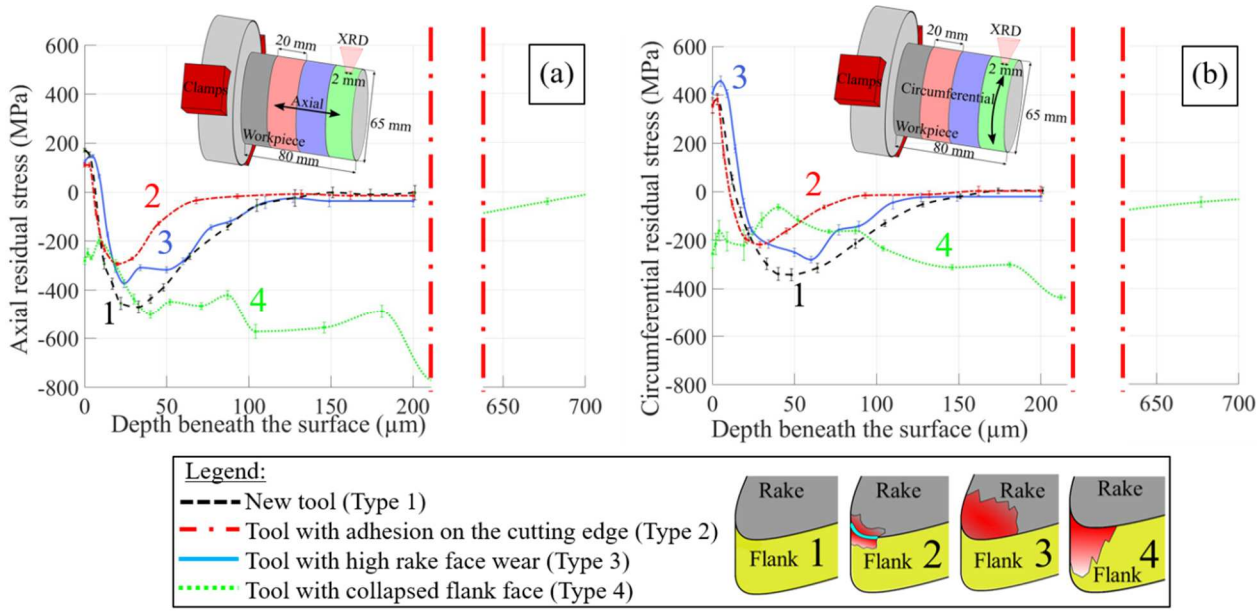

Fig. 5. Experimental residual stresses for the different wear configurations

Tool with rake face wear (Fig. 5 – type 3)

Concerning the tool with the large rake face wear (type B), the impact on the residual stresses is extremely low and could be only due to the precision of the XRD measurements. The wear is probably located too far from the final surface of the workpiece to influence it to a large extent.

Tool with flank wear (Fig. 5 – type 4)

The experimental use of the tool with the collapsed flank face is not realistic, but it can still provide information. Indeed, it can confirm the work of [18] which reported that the affected depth of the residual stresses is directly connected to the evolution of the contact surface between the cutting tool and the machined surface. For this tool, the contact area is around 4.5 times larger than for a new tool, with the machining forces and the affected depth following the same trend.The experimental investigations allow to show the importance of the flank wear and the cutting edge in the residual stresses generation while the impact of the rake face seem to be weak.

The residual stresses are mostly impacted by the part of the tool which is directly in contact with the machined surface like the flank face and the cutting edge. The interaction parameters that evolve with the wear of these surfaces will have a strong impact in the generation of residual stresses.

4. Numerical Simulation

4.1. ALE modeling

The previously reported observations are of interest and provide some trends. However, according to the strong coupling existing in the cutting process, it is difficult to assess the exact mechanisms leading to a change of residual stresses. Especially, it is difficult to extract the contribution of one specific wear type and how this one directly affects the surface integrity.

Residual stresses result of a combination of temperature, temperature gradient and mechanical pressure field. These parameters are mostly controlled by the contact surface zone, which will evolve with the tool wear. At the extreme surface, the levels of temperature create a strong deformation combined with a decrease of the mechanical properties which lead to a tensile stress. On the contrary, more deeply, the temperature is lower and the mechanical properties are less affected and lead to a compressive stress.

As residual stresses are known to be related to the thermomechanical loadings withstood by the surface and sub-surface, a numerical analysis has been performed to observe how they are impacted by the tool wear. Contrary to the experimental process, a numerical approach will allow to isolate a specific phenomenon, such as the impact of the micro-geometry or change in tribological conditions, and simulate a perfectly controlled wear type.

Cutting is simulated in Abaqus explicit via a 2D Eulerian based Arbitrary-Lagrangian-Eulerian (ALE) based on the work of [19] (Fig. 6)

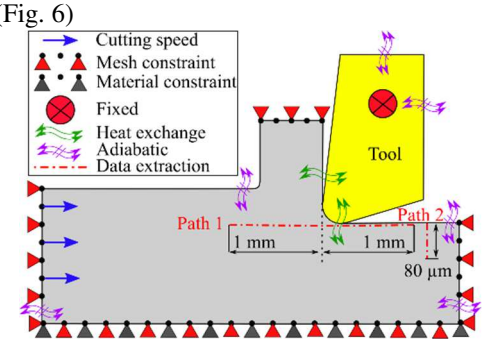

Fig. 6. Boundary conditions of the ALE model and extraction paths of the thermomechanical loadings [19]

The contact between the tool and the workpiece is ensured by a master (tool) / slave (workpiece) with penalty contact method and finite coulomb friction coefficient. The thermal conductance between the tool and the workpiece: 10^4 W/m2.K. The model uses a constant heat partition where the proportion

of the flux going into the workpiece is 0.815. The exchange with the environment is neglected as it is for the radiation loss and the initial temperature of the workpiece and the tool is 20°C.

The tool geometry of this simulation was defined based on the SEM analysis and with a wear willingly exaggerated to facilitate the observation of the results. A Johnson-Cook flow stress model identified by Giovenco [19] has been used to model the 15-5 PH mechanical behaviour, Eq. (1).

$$\sigma_{eq} = \left[A + B \cdot \left(\bar{\varepsilon_p}\right)^n\right] \cdot \left[1 + C \cdot \ln\left(\frac{\dot{\bar{\varepsilon}_p}}{\dot{\bar{\varepsilon}_0}}\right)\right] \cdot \left[1 - \left(\frac{T - T_0}{T_F - T_0}\right)^m\right] \quad (1)$$

A [MPa]	*B* [MPa]	*n*	*m*	*C*	*TF* [°C]	*T0* [°C]
800	650	0,2092	0,93	0,01	1440	20

Table. 1. Johnson-Cook's parameters of the 15-5 PH

The aim of this simulation is to observe the impact of the selected tool wear types on the thermomechanical loadings and observe the evolution of the strain hardening.

To represent the different wear types, four simulations were conducted based on the experimental observation. The geometry was idealised and amplified to simplify the simulation and make the analysis of the results easier:

- The first one represents a new tool with a cutting edge radius of 68 µm. The friction and heat partition coefficients (tool/chip and tool/workpiece), are those of the Al_2O_3 coating identified by Mondelin [6].
- The second simulation uses a tool with a cutting edge supposed rounded due to the wear. The radius of the cutting edge was increased up to 140 µm.
- The third is modelled by a spline with a length of 500 µm and a depth of 25 µm. Tribological conditions in the worn zone are here similar to those selected in previous case.
- The fourth simulates of the flank face wear, the contact length of the tool was increased to 400 µm and with an angle of 3°. in agreement with the work of Ducobu et al. [15]. The friction and heat partition coefficients are corresponding to those of the substrate in contact with the 15-5PH [20].

To allow the chip and the stresses to be stabilized, the model simulates a cutting time of 1.5ms with a mesh size of 12.5µm.

4.2. Analysis

According to the work of Mondelin et al. [6] the principal parameters that influence the generation of residual stresses in the workpiece are the temperature, the normal stress (S22) and the tangential stress (S12) to the surface. These loadings were extracted directly under the tool, on the extreme surface of the workpiece (Fig. 6 path 1). The equivalent plastic strain was observed to compare the evolution of the strain hardening along the depth below the machined surface (Fig. 6 path 2). Indeed, the strain hardening zone is at the origin of the surface residual stresses because these plastic deformations of the surface will induce elastic deformations in the sub-surface. These deformations will create the surface residual stresses [1].

The Fig. 7 plots the evolution of these parameters with the different tool wear types. The A point represents the first point of the tool in contact with the material, B and C points represents respectively the end of the cutting edge of the new tool and the one with the rounded cutting edge. The D point symbolizes the end of the flank face contact of the worn flank face tool.

4.3. Discussion

Contact length

Even if these results need to be taken with caution it can be seen that the evolution of the tool-workpiece contact length induces a large increase in the normal stress peak (Fig 7.b)) and the temperature (Fig 7.c)). The tangential stress (Fig 7.a)) seems to be less impacted by this wear type, with only a larger affected surface but with a lower intensity. The drastic evolution of the normal stress and the temperature, impact considerably the plastic strain (Fig 7.d)) which is 4 times more important than for the new tool. These results are in agreement with the experimental investigations with the tool (C) showing a collapsed flank face, which led to a surface residual stress modification deeper than the other tools and only in compression due the predomination of the mechanical contribution compared to the thermal one.

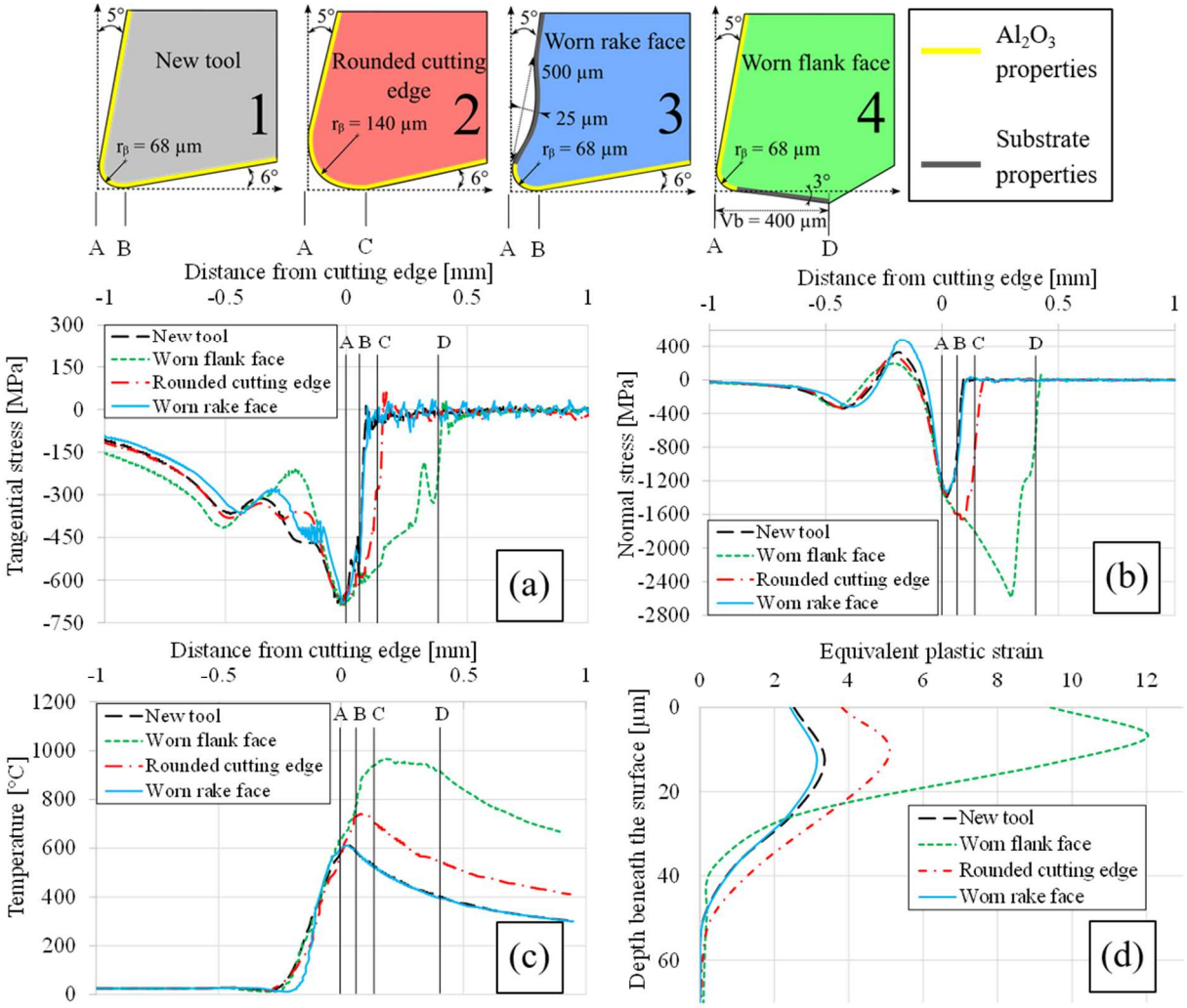

Fig. 7. Numerical thermomecanical loadings induced by the different wear types

Edge radius

An increase in the cutting edge radius (Fig. 7) has a similar impact than the evolution of the flank face wear but with a limited intensity. Both of these micro-geometries evolution can be assimilated to a rise of the contact length. These findings cannot be directly related to the tool A of the experimental campaign which exhibited a different trend. This could be probably due to the fact that the physical phenomenon induced by the material transfer was not properly taken into account. Indeed the 15-5PH doesn't have the same hardness than the tool and will result in a micro-geometry extremely instable during the machining. For the moment this process cannot be handled in the ALE simulation.

Rake face

The simulation with a wear on the rake face showed no impact on the final surface of the workpiece whether in terms of residual stresses, temperatures or plastic strains (Fig. 7). This confirms the trend experimentally observed in the previous section.

5. Conclusion

The first part of this article presented different tool wear types and their impact on the residual stresses. An ALE model was then developed to assess numerically the impact of these wear types on the thermomechanical loadings applied onto the machined surface. Four tools, with different micro-geometries and tribological input data depending on the wear type, were simulated, i) new tool, ii) a tool with a larger cutting edge, iii) a tool with an large wear on the flank face symbolized by an increase of the contact length and iv) a tool with a large wear on the rake face represented by a crater.

With these 4 ALE simulations, it was possible to separate the effect of each wear types and conclude that:

- Increasing the wear on the flank face will have a high impact on the residual stress of the workpiece by increasing the affected deep.
- The evolution of the cutting edge is similar to an increase of the contact length on the flank face but with a lower intensity.

- The rake face wear has no impact on the surface residual stress state and can be neglected.

The exact contribution of the tribological conditions has not really been investigated whereas it could be a major parameter affecting the tool-workpiece interaction and consequently the thermomechanical loadings. The next step related to this work will be thus to characterize independently the tribological properties of each coating against the work material. It could be then possible to refine the physics of the tool-material interaction by applying these friction and heat partition coefficients locally according the level of wear.

Acknowledgments

Authors would like to express their gratitude to AIRBUS HELICOPTERS, FRAMATOME, SAFRAN and CETIM for their financial support.

References

1. Rech J, Hamdi H, Valette S (2008) Rédaction du chapitre 3 dénommé “Surface finish and integrity”, Titre de l’ouvrage édité par J. Paulo Davim : « Machining : fundamentals and recent advances », Springer 2. Springer London, London
2. Smith S, Melkote SN, Lara-Curzio E, et al (2007) Effect of surface integrity of hard turned AISI 52100 steel on fatigue performance. Mater Sci Eng A. https://doi.org/10.1016/j.msea.2007.01.011
3. Jawahir IS, Brinksmeier E, M’Saoubi R, et al (2011) Surface integrity in material removal processes: Recent advances. CIRP Ann - Manuf Technol. https://doi.org/10.1016/j.cirp.2011.05.002
4. Guo YB, Warren AW, Hashimoto F (2010) The basic relationships between residual stress, white layer, and fatigue life of hard turned and ground surfaces in rolling contact. CIRP J Manuf Sci Technol. https://doi.org/10.1016/j.cirpj.2009.12.002
5. Yang X, Richard Liu C, Grandt AF (2002) An Experimental Study on Fatigue Life Variance, Residual Stress Variance, and Their Correlation of Face-Turned and Ground Ti 6Al-4V Samples . J Manuf Sci Eng 124:809–819. https://doi.org/10.1115/1.1511174
6. Mondelin A, Valiorgue F, Rech J, et al (2012) Hybrid model for the prediction of residual stresses induced by 15-5PH steel turning. Int J Mech Sci 58:69–85. https://doi.org/10.1016/j.ijmecsci.2012.03.003
7. Valiorgue F, Rech J, Hamdi H, et al (2012) 3D modeling of residual stresses induced in finish turning of an AISI304L stainless steel. Int J Mach Tools Manuf 53:77–90. https://doi.org/10.1016/j.ijmachtools.2011.09.011
8. Methon G, Valiorgue F, Dumas M, et al (2019) Development of a 3D hybrid modeling of residual stresses induced by grooving. Procedia CIRP 82:400–405. https://doi.org/10.1016/j.procir.2019.04.002
9. Attanasio A, Ceretti E, Giardini C (2009) 3D FE modelling of superficial residual stresses in turning operations. Mach Sci Technol 13:317–337. https://doi.org/10.1080/10910340903237806
10. Kortabarria A, Arrazola PJ, Ostolaza K (2013) Multi revolution finite element model to predict machining induced residual stresses in inconel 718. In: Procedia CIRP
11. Madariaga A, Kortabarria A, Hormaetxe E, et al (2016) Influence of Tool Wear on Residual Stresses When Turning Inconel 718. Procedia CIRP 45:267–270. https://doi.org/10.1016/j.procir.2016.02.359
12. Chen L, El-Wardany TI, Harris WC (2004) Modelling the effects of flank wear land and chip formation on residual stresses. CIRP Ann - Manuf Technol 53:95–98. https://doi.org/10.1016/S0007-8506(07)60653-2
13. Liu M, Takagi JI, Tsukuda A (2004) Effect of tool nose radius and tool wear on residual stress distribution in hard turning of bearing steel. J Mater Process Technol 150:234–241. https://doi.org/10.1016/j.jmatprotec.2004.02.038
14. Muñoz-Sánchez A, Canteli JA, Cantero JL, Miguélez MH (2011) Numerical analysis of the tool wear effect in the machining induced residual stresses. Simul Model Pract Theory 19:872–886. https://doi.org/10.1016/j.simpat.2010.11.011
15. Ducobu F, Arrazola PJ, Rivière-Lorphèvre E, Filippi E (2015) Finite element prediction of the tool wear influence in Ti6Al4V machining. In: Procedia CIRP
16. Trent EM, Wright PK (2000) Metal Cutting Fourth Edition
17. Tang L, Sun Y, Li B, et al (2019) Wear performance and mechanisms of PCBN tool in dry hard turning of AISI D2 hardened steel. Tribol Int. https://doi.org/10.1016/j.triboint.2018.12.026
18. Kermouche G, Rech J, Hamdi H, Bergheau JM (2010) On the residual stress field induced by a scratching round abrasive grain. Wear. https://doi.org/10.1016/j.wear.2010.03.012
19. Giovenco A (2018) Contribution à la simulation numérique de l ’ usure des outils de coupe Remerciements
20. Mondelin A (2012) Thèse de l ’ Université de Lyon Modélisation de l ’ intégrité des surfaces usinées Application au cas du tournage finition de l’acier inoxydable 15-5PH